Chapter

Characteristics of Eco-friendly Kenaf Fiber-Imbedded Nonwoven for Automotive Application

Seung Jin Kim and Hyun Ah Kim

Abstract

This study examined the physical properties of kenaf fiber-imbedded nonwoven for automotive pillar trim according to the blend ratio of the fibers and needle-punching process conditions. Kenaf-imbedded nonwoven specimens mixed with polypropylene (PP) and low-melt PET (LM PET) fibers were prepared via needle-punching, and their physical properties such as air permeability, water absorption, sound absorption coefficient, and porosity were investigated according to the various processing conditions. The kenaf-imbedded nonwoven treated with high needle depth in the needle-punching process and/or mixed with a large amount of LM PET exhibited the highest breaking and tearing strengths, due to the high weight of the nonwoven specimens. A high blend percentage of LM PET fibers reduced the pore size, which resulted in low air permeability and water absorption. The sound absorption coefficient of the kenaf-imbedded nonwoven specimens was highly dependent on its weight and thickness. Regarding the lamination treatment, the laminated nonwoven exhibited higher breaking and tearing strengths, thermal conductivity, and sound absorption coefficient than the non-treated one. In addition, the HDPE powder-treated nonwoven exhibited lower breaking and tearing strengths, air permeability, water absorption, and sound absorption, due to the reduced pore size.

Keywords: kenaf, needle-punching, low-melt PET, sound absorption coefficient porosity, fogging

1. Introduction

The scientific name of kenaf is *Hibiscus cannabinus* L. The principal ingredients of kenaf fiber are cellulose, lignin, and pectin, and the hemicellulose distribution ranges between 10 and 22% according to the type of kenaf fiber. Research on the application to fashion textile materials with soft tactile hand by retting treatment of kenaf stem has been conducted by Ramaswamy et al. [1], Tao et al. [2], and Lee et al. [3, 4]. In particular, many studies have examined the spinning and fabric manufacturing technology using mixed fibers with cotton and kenaf, including Bel-Berger et al. [5], Weiying et al. [6], and Zhang [7]. Advanced composite materials mixed with kenaf and natural fibers with light weight, VOC-free, and good abrasion resistance are needed nowadays and have been studied for eco-friendly automotive materials [8–10]. In addition, the use of kenaf fiber in nonwoven

was investigated by Moreau et al. [11], Yang et al. [12], and Tao et al. [13, 14]. Nonwoven has been used in the various industries because of its advantages of fast processing and competitive price. Recently, nonwoven has become one of the most common textile products in the automotive industry with sound absorption properties. The nonwoven fabrics used in the automotive industry require high functional quality and reliability. Many studies have examined the sound absorption property, including physical properties such as air permeability and wicking, of nonwovens. The studies carried out using natural jute [15] and coconut coir [16] fibers yielded good sound absorption properties. Kenaf, jute, and cotton fiber-imbedded nonwovens with PET and polypropylene (PP) fibers were used as industrial automotive padding materials and have significantly improved the sound absorption properties [17]. Nick et al. [18] investigated the acoustic behavior using three different composite materials: (1) cotton, bicomponent PET, and PP fibers; (2) flax, hemp, and PP fibers; and (3) lyocell, bicomponent PET, and PP fibers. The third composite material with lyocell fibers of 0.9 dtex exhibited the best sound absorption property. Lou et al. [19] studied the sound absorption property of nonwoven composed of low-melt PET (LM PET) and recycled PET particles mixed with PP fibers. The thick and low-density nonwoven specimens exhibited high sound absorption coefficients at low- and mid-frequency sound ranges. Lee et al. [20] examined the relationship between the acoustic absorption values of the recycled polyester nonwovens and the nonwoven processing conditions, including fiber and web properties. Byun et al. [21] investigated the sound absorption property of the PET nonwoven for automotive application according to the variation of the fiber fineness, density, and thickness of the three-layer nonwoven by substituting glass wool in order to improve the environmental and recycled capability. Kücük and Korkmaz [22] examined the effects of the physical parameters on the sound absorption properties of natural fiber-mixed nonwoven fabrics. They concluded that an increased thickness and decreased air permeability resulted in an increase of sound absorption properties. In addition, an increased amount of fiber per unit area resulted in an increase in sound absorption. On the other hand, Dubrovski and Brezocnik [23] studied the effects of the content of viscose and PET fibers and the porosity of the nonwoven structure on the vertical wicking rate of nonwovens. The results showed that higher-volume porosity gives higher vertical wicking rate. Soukupova et al. [24] studied the effect of the blend ratio of viscose and PET fibers on the wicking of the nonwoven and found that the capillary rise was higher for nonwoven fabrics containing more viscose fibers. Dubrovski and Brezocnik [25] predicted the model for the vertical wicking rate using the fiber density, fiber fineness, and nonwoven fabric density. Das et al. [26] and Tascan and Vaughn [27] examined the influence of fiber cross-sectional shape on the air permeability of nonwoven. Das et al. [26] found that the air permeability decreased with a higher proportion of noncircular fibers in the nonwoven fabrics, which was similar to Tascan and Vaughn's results [27].

In previous studies, LM PET and PP fibers as nonwoven materials were mixed with natural fibers such as cotton, lyocell, flax, jute, and coconut coir to enhance their physical properties such as the wicking rate, air permeability, and sound absorption property for automotive-acoustic materials. However, no detailed study has yet examined the physical properties of the kenaf fiber-imbedded nonwoven. Therefore, in this study, kenaf fiber-imbedded nonwoven specimens were produced with different processing conditions such as number of carding treatments, web layers, needle depth, and content ratio of LM PET, and their physical properties such as air permeability, water absorption, and sound absorption coefficient were measured in order to optimize the processing conditions for automotive pillar trim. Furthermore, the correlation between the breaking and tearing strengths and the

structural factors of the nonwoven were investigated according to the processing conditions. In addition, the effect of different processing conditions on the fogging value of the nonwoven was investigated.

2. Experimental

2.1 Specimen preparation

Kenaf, PP, and LM PET were used as raw materials of the nonwoven. **Table 1** presents the physical properties of the kenaf, PP, and LM PET staple fibers used. Ten kinds of kenaf-imbedded nonwoven specimen as a first batch of specimen were made with different processing conditions, as shown in **Table 2**.

Figure 1 shows the needle-punching nonwoven process to prepare the specimens. **Figure 2** shows an image of the nonwoven machinery used. Three types of staple fiber supplied from material supply equipment were mixed and blended in the mixing tank shown in **Figure 1**. Specimen 1 in **Table 1** was mixed and blended by single opener in the mixing tank, and specimens 2–10 were prepared by multi-opener.

As shown in **Table 2**, the basic blend ratio of kenaf, PP, and LM PET staple fibers was 40, 40, and 20%, respectively (specimens 1–9). The blend ratio of specimen 10 was changed to 30, 30, and 40%. The mixed and blended fibers were delivered to the first and second carding processes. The basic carding treatment was conducted twice, but specimen 4 underwent only one treatment. Lap forming was performed after the carding process. The layering of the carding lap was changed from two to four layers, as shown in **Table 2**. The needle-punching process was followed by the second web-forming process, as shown in **Figure 1**. The basic needle depth was 16 mm, but specimens 7 and 8 had a needle depth of 18.6 and 14.4 mm, respectively. The specimens underwent thermo-compression bonding after the needle-punching process, as shown in **Figure 1**. Polyethylene (PE) powder was added after the thermo-bonding process to enhance coherence between the fabric and PP foam when automotive pillar trim was fabricated, as shown in **Figure 3**. **Figure 3** shows the pillar trim in automotive interior. Kenaf-imbedded nonwoven is located between PP foam and fabric, which is placed on the inside of automotive pillar trim. Fabric is usually made by polyester (cation dyeable polyester).

Hot melt film was inserted between the fabric and the kenaf-imbedded nonwoven to enhance the adhesive force between them. In addition, the reason why low-melting (LM) PET is mixed to make nonwoven is to enhance the adhesive force among hot melt film, fabric, and kenaf-imbedded nonwoven.

Physical properties	Kenaf	Low-melting PET (LM PET)	Polypropylene (PP)
Fiber length (mm)	64.8	51.8 ± 5.0	64
Linear density (d)	8	4.53 ± 0.41	8 ± 0.5
Maker/origin	Bangladesh	Toray Chemical	Han Kook Fiber Co. Ltd
Breaking strength (gf/d)	4	3.52 ± 0.42	4 ± 0.5
Breaking strain (%)	200	44.0 ± 8.7	200 ± 20
Moisture regain (%)	11.8	—	0.1

Table 1.
Physical properties of staple fibers used.

No.	Blend ratio (kenaf:PP:LM PET)		No. of carding treatment	Layer of web	Needle depth	Thermal compression bonding	Powder treatment
1	Single opener	40:40:20	3 Layers	3 Layers	16 mm	O	O
2	Multi-opener	40:40:20	3 Layers	3 Layers	16 mm	O	O
3		40:40:20	3 Layers	3 Layers	16 mm	O	X
4		40:40:20	3 Layers	3 Layers	16 mm	O	O
5		40:40:20	4 Layers	4 Layers	16 mm	O	O
6		40:40:20	2 Layers	2 Layers	16 mm	O	O
7		40:40:20	3 Layers	3 Layers	18.6 mm	O	O
8		40:40:20	3 Layers	3 Layers	14.4 mm	O	O
9		40:40:20	3 Layers	3 Layers	16 mm	X	O
10		30:30:40	3 Layers	3 Layers	16 mm	O	O

Table 2.
Processing conditions for ten kinds of kenaf-imbedded specimen.

Therefore, to examine the effect of the polyurethane (PU)-laminating film treatment on the thermal conductivity, water absorption, and sound absorption properties of the kenaf-imbedded nonwoven, a second batch of specimens was prepared by the same procedure as that for the first batch. **Table 3** presents the eight types of nonwoven specimen as a second batch of specimens. Two types of specimen were prepared as nonlaminated (1–4) and laminated (5–8) by PU film. The blend ratio of kenaf, PP, and LM PET staple fibers was 40, 40, and 20% as a fixed blend ratio. The carding treatment was conducted twice, and the number of layers of the carding lap was fixed at three. The needle depth was fixed at 16 mm. In the thermo-compression bonding process, the surface temperature of the bonding roller was set at 170°C, and its velocity was fixed at 7.2 m/min. Specimens 1 and 3 were treated with powder after the thermo-compression bonding process and have different weight. Specimens 2 and 4 were non-treated and also have different weight. Specimens 5–8 were laminated by PU film after the needle-punching nonwoven process. The temperature of the laminating roller was 129°C, and the

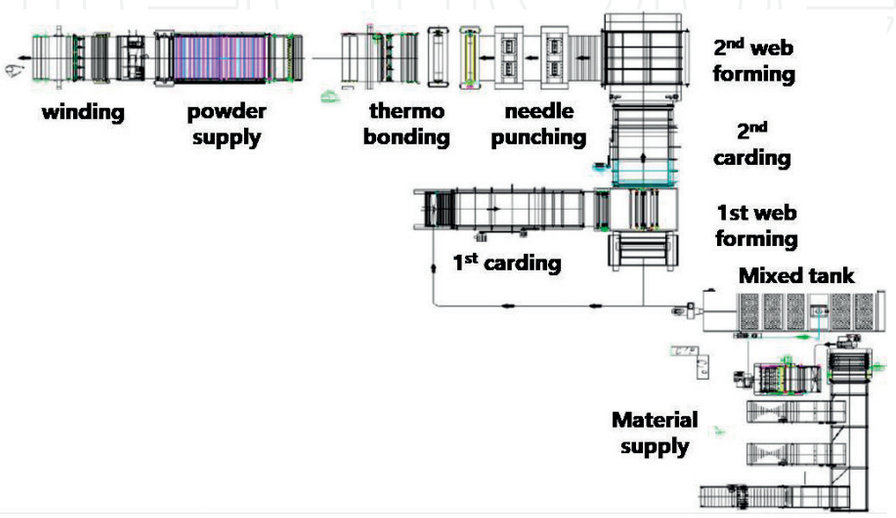

Figure 1.
Needle-punching nonwoven process.

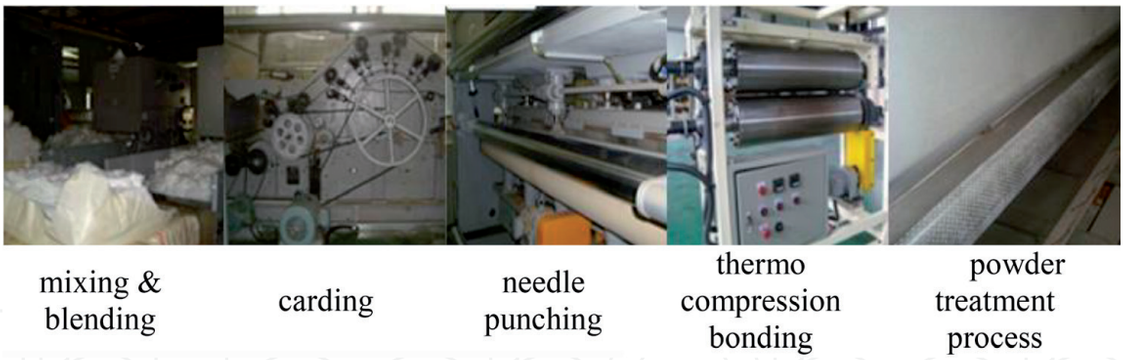

Figure 2.
Image of the nonwoven machinery.

doting temperature on the melting apparatus was set at 126°C and the feed speed of the laminating roller at 3.7 m/min. After laminating by PU film, aging was carried out at 60% of RH in the aging room for 24 hours.

2.2 Measurement of physical properties

2.2.1 Tensile and tearing strengths

The breaking strength and strain of the nonwoven specimens were measured using Testometric apparatus (Model Micro 350, England) according to KSK ISO 9073-3: 2009. A specimen of width 50 mm and length 200 mm was prepared and elongated at a speed of 100 mm/min. The tearing strength of the nonwoven specimens was measured using Testometric apparatus (Model Micro 350, England) according to KSK ISO 9073-4: 2010. A specimen of width 75 and length 150 mm was prepared. In addition, the breaking strength, strain, and initial modulus of the nonwoven specimens prepared at machine direction (MD) intervals of 30 degrees were measured. The preparation of the specimens is shown in **Figure 4**. Furthermore, the orientation factor of fibers in the nonwoven specimens was calculated as the measured inclined angle (θ) of the 500 fibers in the nonwoven fabric as shown in **Figure 5**, and the distribution of the measured angles was analyzed in relation to the measured tensile property.

2.2.2 Thickness

The thickness of the ten (first batch specimen) and eight (second batch specimen) different nonwoven specimens was measured using the FAST-1 system. **Figure 6** shows an image and schematic diagram of the compression meter by FAST-1 system [28]. The thickness (mm) at a compression force of 2 gf/cm^2 was measured, and 30 assessments of each specimen were carried out for calculating the mean thickness.

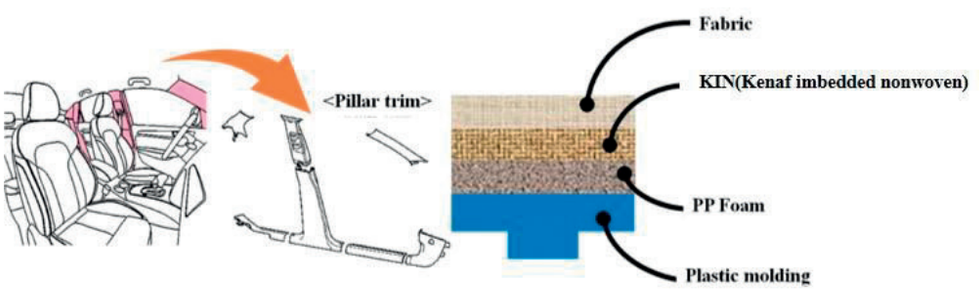

Figure 3.
Schematic diagram of pillar trim.

No.	Lamination	Kenaf:PP:LM PET (blend ratio)	No. of carding treatment	Layer of web	Needle depth	Thermo-compression bonding roller treatment	Powder treatment	Weight (g/m^2)	Thickness (mm)
1	Nonlaminated	40:40:20	2	3 layers	16 mm	170°C, 7.2 m/min	o	240	0.60
2		40:40:20	2	3 layers	16 mm	170°C, 7.2 m/min	X	240	2.10
3		40:40:20	2	3 layers	16 mm	170°C, 7.2 m/min	o	320	0.82
4		40:40:20	2	3 layers	16 mm	170°C, 7.2 m/min	X	320	2.75
5	Laminated by PU film	40:40:20	2	3 layers	16 mm	170°C, 7.2 m/min	o	420	1.34
6		40:40:20	2	3 layers	16 mm	170°C, 7.2 m/min	X	420	2.53
7		40:40:20	2	3 layers	16 mm	170°C, 7.2 m/min	o	500	1.53
8		40:40:20	2	3 layers	16 mm	170°C, 7.2 m/min	X	500	3.17

Note: o, treated; x, non-treated.

Table 3.
Preparation of the eight kinds of kenaf-imbedded specimen.

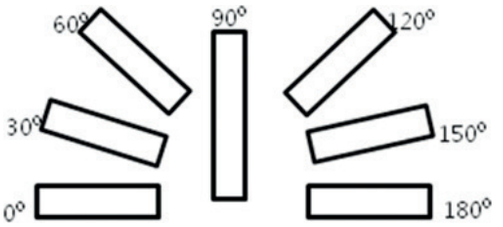

Figure 4.
Preparation of specimens for measuring tensile property of nonwoven fabric.

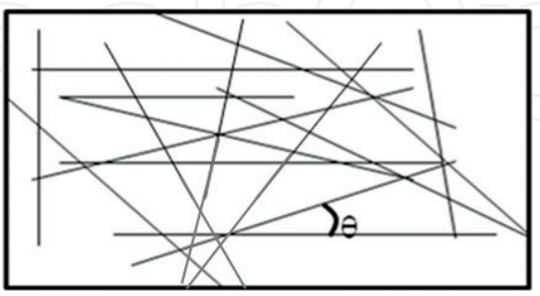

Figure 5.
Measured orientation angle of the fibers in the nonwoven.

2.2.3 Porosity

The pore size (diameter, D, μm) was measured using a capillary flow porometer (CFP-1200AE PMI Co., USA). The measured pore diameter (D) was calculated using Eq. (1) with the median value of the graph between the air flow and pressure. The mean and largest pore diameters were measured for each specimen:

$$\text{Pore diameter (D)} = \frac{C\tau}{\rho} \tag{1}$$

where C is a constant, τ the surface tension of the liquor (dyne/cm), and ρ the pressure (1b/(in)^2). **Figure 7** shows the capillary flow porometer.

2.2.4 Air permeability

The air permeability (R) was measured using Fx3300 (TEXTEST, Switzerland) according to the KSK ISO 9237 method. An air pressure of 100 Pa was applied to a 20 cm^2 area of the specimen, and the air permeability was calculated using the following Eq. (2). **Figure 8** shows the air permeability measuring apparatus:

$$\text{Air permeability (R, cm3/cm2/g)} = \frac{Q}{A} \times 167 \tag{2}$$

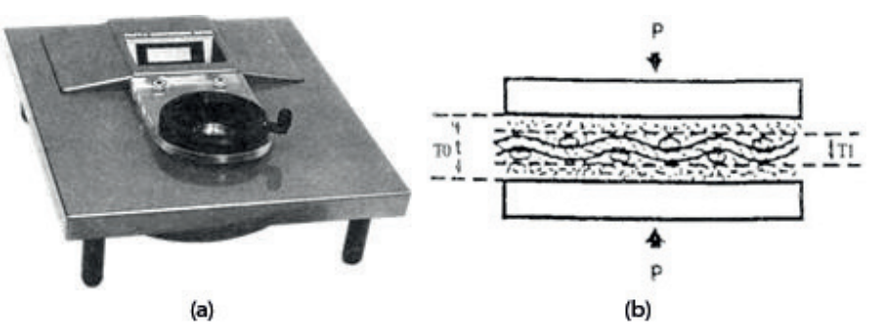

Figure 6.
FAST-1 system for measuring compressibility [28]. (a) Image of FAST-1 and (b) Schematic diagram.

Figure 7.
Image of capillary flow porometer, CFP-1200AE.

where Q is the arithmetic mean of air flow (cm^3/min), A the area of the specimen (cm^2), and 167 the conversion constant.

2.2.5 Water absorption property

The water absorption property was assessed by KSK ISO 9073-6. The liquid absorption capacity (LAC) was calculated by Eq. (3):

$$\text{LAC} = \frac{\text{weight of specimen absorbed (B)} - \text{weight of dried specimen (A)}}{\text{weight of dried specimen (A)}} \times 100 \qquad (3)$$

A square specimen of dimensions 100 mm × 100 mm was prepared and conditioned under 20 ± 1°C and 65 ± 5% RH. After its dry weight (A) was measured, the specimen was submersed to a depth of 20 mm in the water bath for 60 s, then taken out, and hung horizontally for 120 s, and finally its weight (B) was measured again, and LAC was calculated by Eq. (3) as the average value of five measurements.

2.2.6 Sound absorption property

The sound absorption coefficient of the nonwoven specimen was measured using acoustic duct (SCIEN-9301, USA) according to KSF2814-2: 2002. **Figure 9** shows the acoustic duct apparatus.

Figure 8.
Image of FX 3300.

Figure 9.
Acoustic duct, SCIEN-9301. (a) Low Frequency and (b) High Frequency.

The specimen was fastened at the impedance tube's left wall, and a loudspeaker was attached at its right wall. Sound waves of well-defined frequencies were emitted by a loudspeaker. The nodes and antinodes of the standing waves emitted from the loudspeaker and those reflected from the specimens were detected by two small microphones, from which the sound absorption coefficient was calculated by frequency response transfer function from two microphone channels. The frequency used was between 100 and 1600 Hz for low frequency and between 500 Hz and 6.3 kHz for high frequency.

2.2.7 Measurement of thermal conductivity

The thermal conductivity (K) of the nonwoven specimen was measured using KES-F7 (Thermolabo, Kato Tech. Co. Ltd., Japan) and calculated using Eq. (4):

$$Q = K\frac{A \cdot \triangle T}{d} \tag{4}$$

where Q is the heat loss (W/cm^2), d the specimen thickness (cm), A the area of the specimen (cm^2), and ΔT the temperature difference. **Figure 10** shows an image of the KES-F7 measuring apparatus.

2.2.8 Fogging test

A fogging test of the nonwoven specimen was performed to examine the emission of volatile organic compounds (VOC) using the gravimetric method according to KSM ISO 6452. A circular specimen of diameter 80 ± 1 mm was prepared and put

Figure 10.
Image of the KES-F7 measuring apparatus.

into a thermostatic bath covered with aluminum foil which was boiled for 16 hours at 100°C. The fogging value was calculated using the mass of aluminum foil wrapped on the beaker in the thermostatic bath before and after the experiment.

2.2.9 Measurement of the surface texture of the nonwoven

The surface texture of the nonwoven specimen was measured by SEM (S-4300, Hitachi Co., Japan) and optical microscopy (I Camscope 305A, Korea).

3. Results and discussion

3.1 Physical properties of kenaf-imbedded nonwoven according to the processing conditions

3.1.1 Breaking and tearing strengths of the nonwoven

Table 4 lists the physical properties of the ten kinds of nonwoven specimen.

Figure 11(a) and **(b)** shows the breaking and tearing strengths of the nonwoven specimens. Specimens 3 and 10 showed the highest breaking and tearing strengths. As shown in **Table 4**, specimens 3 and 10 had a smaller mean pore size and higher weight than the other specimens. Therefore, the effect of the mean pore size and weight on the breaking and tearing strengths of the nonwoven was investigated. **Figure 12** shows a diagram of the breaking and tearing strengths according to the weight of the nonwoven specimens.

The breaking and tearing strengths of the MD and CD direction of the nonwoven specimen were increased with increasing weight of the nonwoven. This was attributed to the more numbers of fibers per unit area in the nonwoven specimens according to the increase of weight, which results in higher breaking and tearing strengths due to the more contribution of the fibers to the resistance from external load. **Figure 13** shows a diagram of the breaking and tearing strengths according to the mean pore size. The breaking and tearing strengths of the nonwoven specimens were decreased with increasing mean pore size of the nonwoven specimen, possibly due to the weakened resistance from external force due to the large pore size in the nonwoven. In addition, the breaking and tearing strengths of nonwoven specimen 2, as shown in **Figure 11**, were the lowest, which was attributed to its lowest weight and largest mean pore size as shown in **Table 4**.

On the other hand, the orientation factor and the distribution of the fibers in the nonwoven specimens were measured and discussed to examine their effect on the breaking and tearing strengths of the nonwoven. **Figure 14** presents the fiber orientation distribution of the ten types of nonwoven specimen.

As shown in **Figure 14**, the fiber orientation distributions of specimens 1, 2, 6, and 8 exhibited the shape of a quasi-Gaussian distribution, whereas that of specimens 3 and 10 exhibited a double quasi-normal distribution. Furthermore, specimens 4, 5, 7, and 9 exhibited a random distribution of fiber orientation in the nonwoven, i.e., the number of fibers according to the orientation angle was randomly distributed. As shown previously in **Figure 11**, specimens 3 and 10 exhibited the highest tearing and breaking strengths, respectively, whereas specimen 2 showed the lowest breaking and tearing strengths. This means that the fiber distribution in the nonwoven does not directly affect the breaking and tearing strengths, because specimen 2 with high distribution of fibers between 60° and 120° as a normal distribution exhibited low breaking strength, but specimens 1, 6, and 8 with the same normal distribution as specimen 2 showed higher breaking strength than that of the specimen 2. Furthermore, it was assumed

Specimen no.	Breaking strength (kgf/mm^2)		Tearing strength (N)		Air permeability ($cm^3/cm^2/g$)	Water absorption (%)	Sound absorption coefficient	Mean pore size (μm)	Largest pore diameter (μm)	Thickness (mm)	Weight (g/m^2)
	MD	CD	MD	CD							
1	22.6	22.9	27.0	27.7	51.4	48.7	0.12	34.6	414.4	0.739	254.6
2	9.9	11.2	21.5	25.5	238	55.2	0.14	105.3	407.6	0.713	209.8
3	38.4	40.5	41.9	55.5	26.0	51.3	0.25	38.6	402.5	0.942	363.6
4	21.8	24.1	26.7	32.6	58.9	44.3	0.11	50.5	177.4	0.554	245.8
5	19.7	20.8	26.5	25.9	69.2	72.7	0.11	62.3	408.4	0.598	245.6
6	22.0	30.0	27.2	27.1	59.3	65.4	0.1	73.4	211.9	0.636	251.4
7	21.2	23.4	25.0	29.5	64.9	50.5	0.12	35.8	157.0	0.738	234.2
8	18.1	19.8	24.0	26.6	125.6	59.3	0.1	61.9	256.3	0.632	221.2
9	26.2	22.3	25.3	30.7	89.9	41.7	0.11	68.0	556.4	0.557	258.4
10	41.3	44.8	30.3	44.3	37.6	37.4	0.14	51.0	114.4	0.597	300

Note: MD, machine direction; CD, cross direction.

Table 4.
Physical properties of the nonwoven specimens (first batch of specimens).

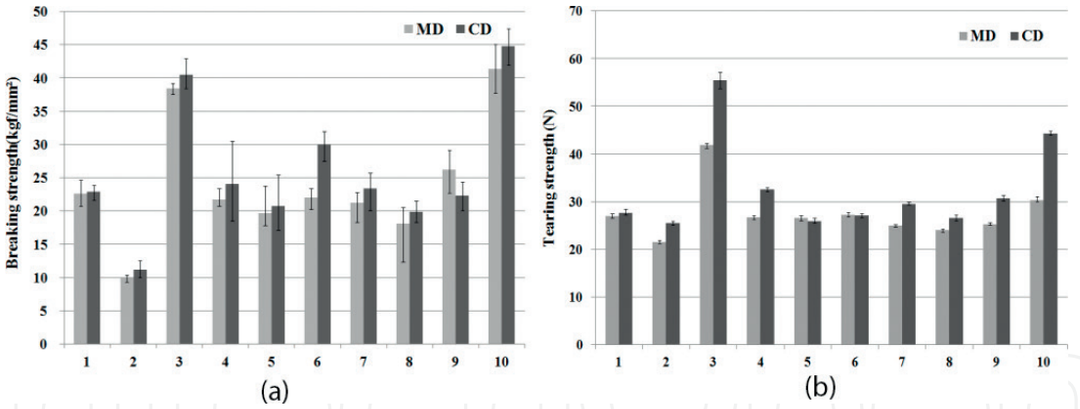

Figure 11.
Breaking and tearing strengths of the nonwoven specimens. (a) Breaking strength and (b) Tearing strength.

that high breaking and tearing strengths of specimens 3 and 10, which showed a double quasi-normal distribution, were attributed to the processing conditions of nonwoven. In addition, the breaking and tearing strengths of nonwoven specimen 2 were measured and discussed according to the cut direction of the nonwoven specimens. **Figure 15** shows the tensile property of specimen 2 according to the cut direction of the specimen. The breaking strength, breaking strain, and initial modulus of the specimens cut along MD, i.e., perpendicular to the cross direction (CD), exhibited maximum values, which was attributed to the many fibers distributed and oriented perpendicular to the CD.

3.1.2 Air permeability

Figure 16(a) presents the air permeability and mean pore size of the nonwoven specimens. Specimens 2 and 8 showed high air permeability, which was attributed to the large pore size and low weight of the nonwoven, as shown in **Table 4**. These specimens were processed under the double-carding treatment in the multi-opener with three

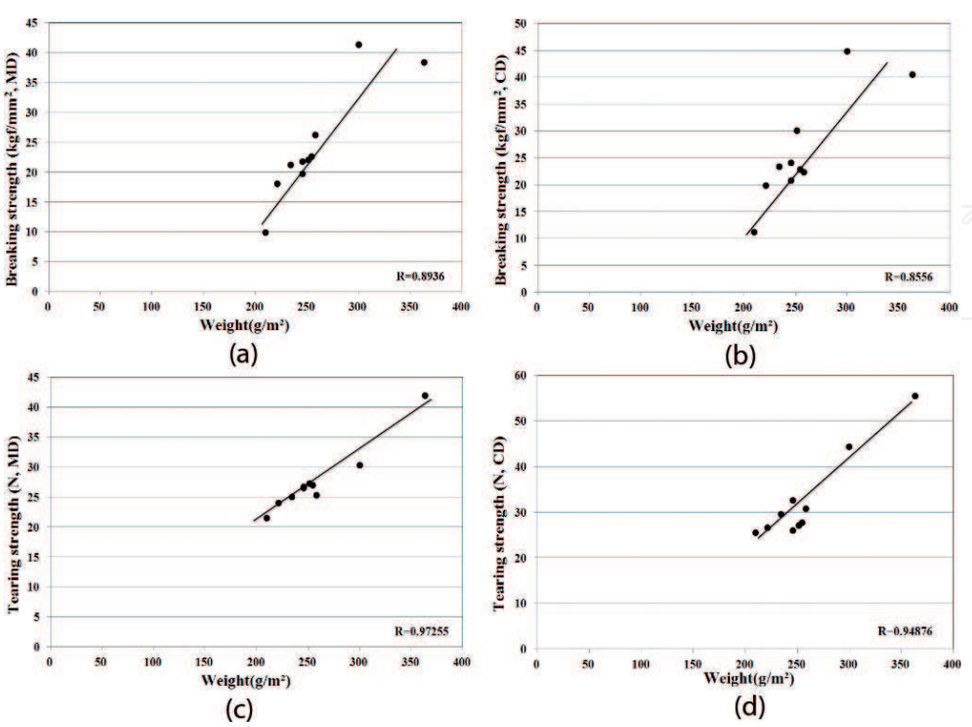

Figure 12.
Diagram of the breaking and tearing strengths according to the weight of the nonwoven specimens. (a) Breaking strength (MD) vs weight, (b) Breaking strength (CD) vs weight, (c) Tear strength (MD) vs weight and (d) Tear strength (CD) vs weight.

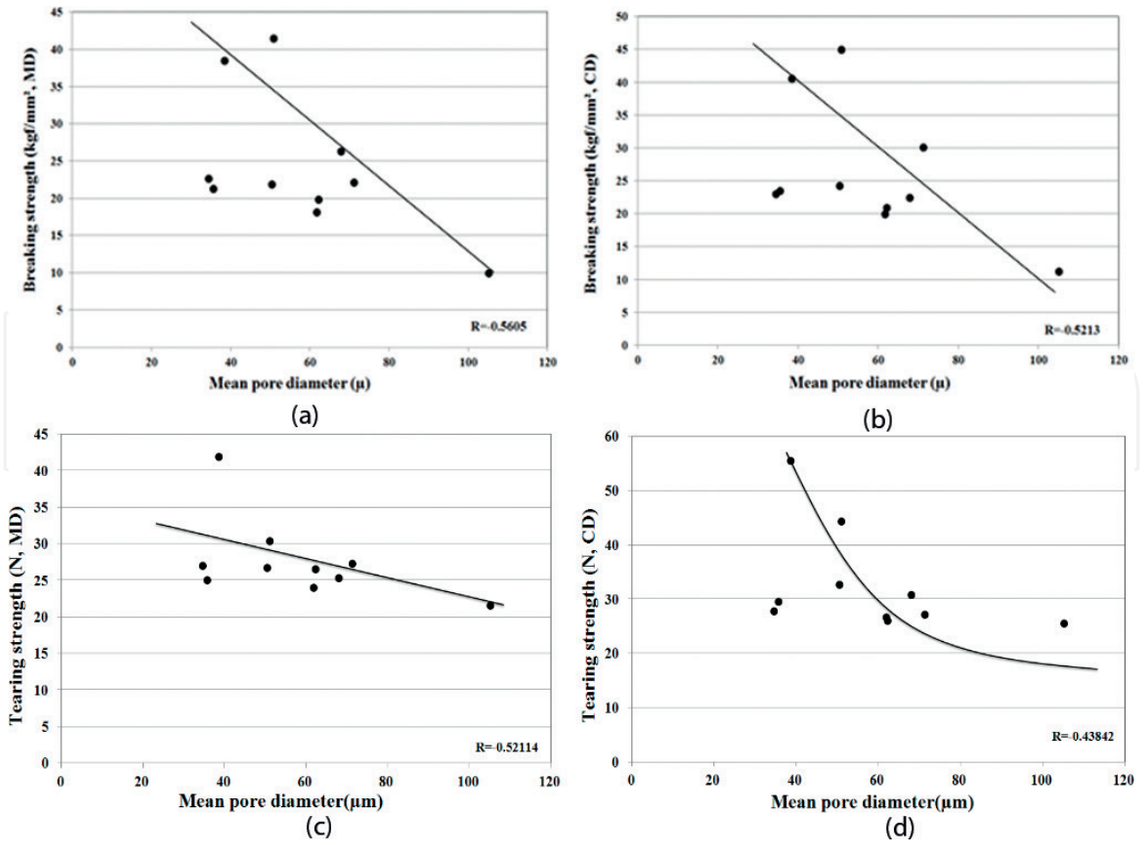

Figure 13.
Diagram of the breaking and tearing strengths according to the mean pore size of the nonwoven specimens. (a) Breaking strength(MD) vsmean pore size, (b) Breaking strength(CD) vsmean pore size, (c) Tear strength(MD) vsmean pore size and (d) Tear strength(CD) vsmean pore size.

layers of web and needle depth of 16 or 14.4 mm. According to two previous studies [26, 27], nonwoven prepared using circular cross-sectional fibers exhibited the highest air permeability than nonwoven with noncircular fiber cross section, which was attributed to the highest pore diameter of nonwoven with circular fibers. These results were similar to our own. **Figure 16(b)** shows a correlation diagram between the mean pore diameter and air permeability of the ten different nonwoven specimens. The air permeability was highly dependent on the mean pore diameter of the nonwoven, and the correlation coefficient between the two parameters was 0.85, which was relatively high.

3.1.3 Water absorption

Figure 17 shows the LAC of the nonwoven specimens. Specimens 2, 5, 6, and 8 showed high liquid absorption, which was related with their large mean pore size. Furthermore, specimens 2, 5, 6, and 8 had larger pore diameter than specimens 4, 7, and 9, as shown in **Table 4**. In particular, the air permeability (**Figure 16**) and liquid absorption (**Figure 17**) of specimen 10 were the lowest, which was attributed to its high percentage of LM PET, i.e., the voids in the nonwoven were blocked by the LM PET that was heat melted on the thermo-compression bonding roller, which shrunk the voids and reduced the air and water flows and hence reduced the air permeability and liquid absorption. According to a previous study [27], high-volume porosity gives high vertical wicking rate, which was a similar result to our own.

3.1.4 Sound absorption coefficient

Figure 18(a) and **(b)** presents the sound absorption coefficient according to the high frequency between 500 and 6300 Hz and the average sound absorption coefficient

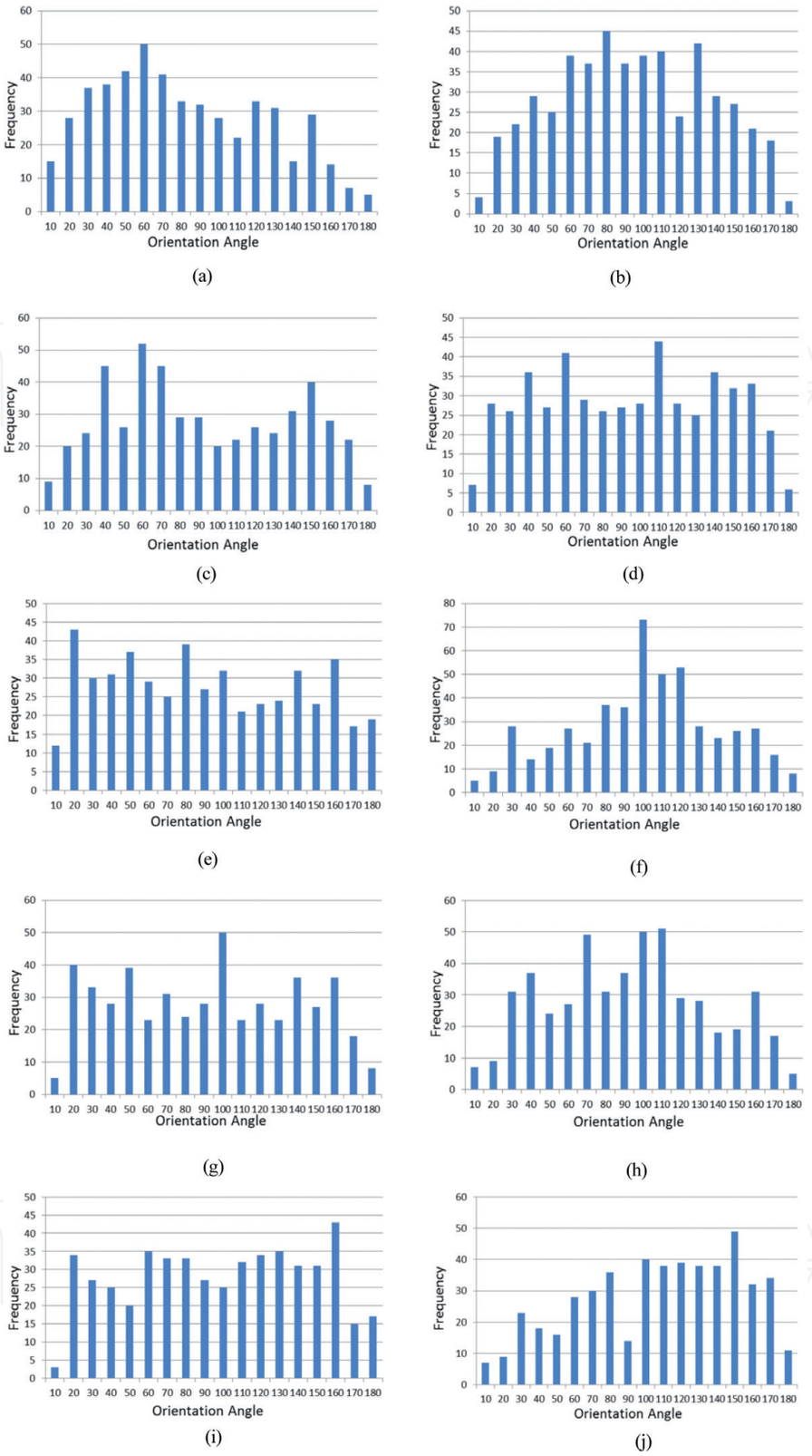

Figure 14.
Orientation of the fibers in the nonwoven specimens. (a) specimen 1, (b) specimen 2, (c) specimen 3, (d) specimen 4, (e) specimen 5, (f) specimen 6, (g) specimen 7, (h) specimen 8, (i) specimen 9 and (j) specimen 10.

of the nonwoven specimens, respectively. Specimens 2, 3, and 10, which had either high thickness and low weight or low thickness and high weight, showed a high sound absorption coefficient. The sound absorption coefficient under high frequency was highly dependent on the thickness and weight of the nonwoven and also partly affected by the pore diameter [19–21]. The sound absorption coefficient of specimen 3 was the largest, which was attributed to its high weight and low pore diameter.

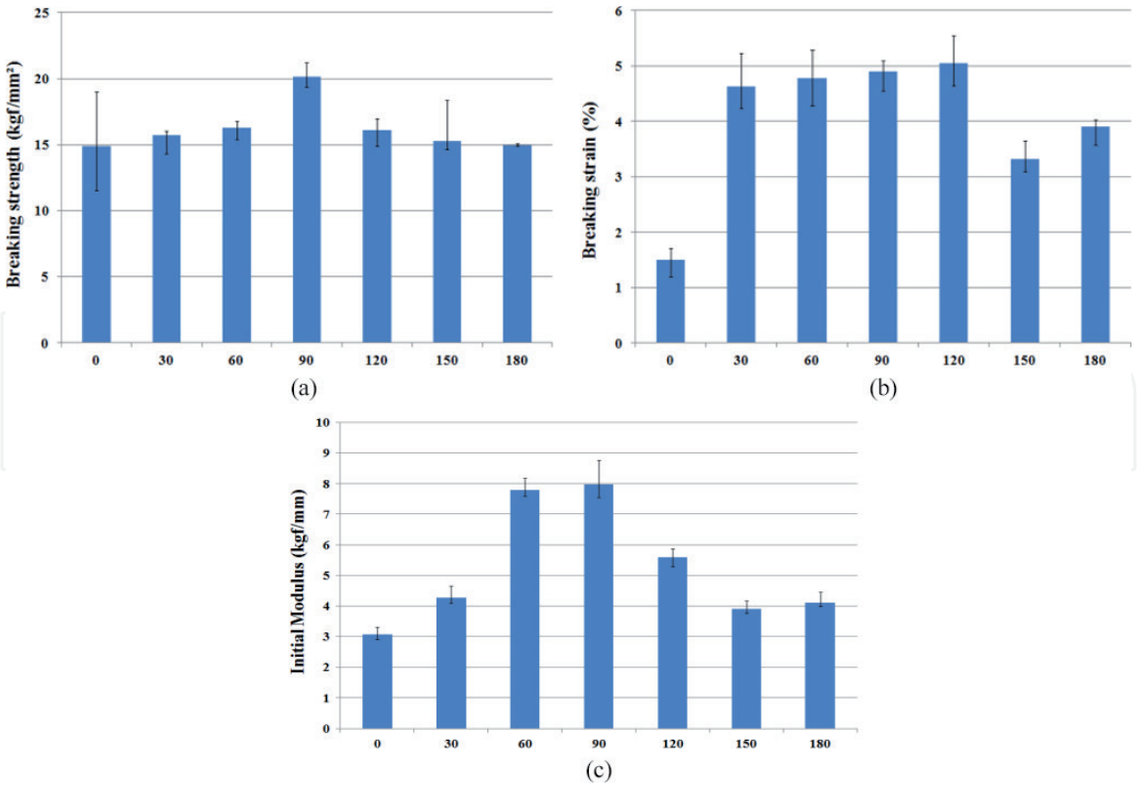

Figure 15.
Tensile property of the specimen (no. 2). (a) Breaking strength, (b) Breaking strain and (c) Initial modulus.

Table 5 shows the correlation coefficient between the sound absorption coefficient under high frequency and the thickness and weight of the kenaf-imbedded nonwoven specimens. The sound absorption coefficient was highly correlated with

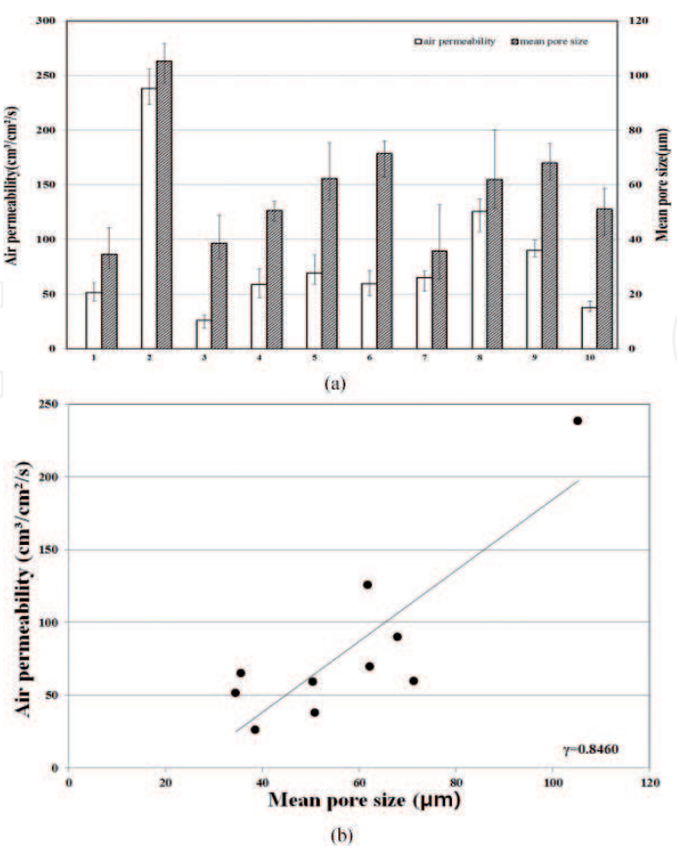

Figure 16.
Air permeability of the nonwoven specimens. (a) Air permeability of each specimens and (b) Air permeability vs Mean pore size.

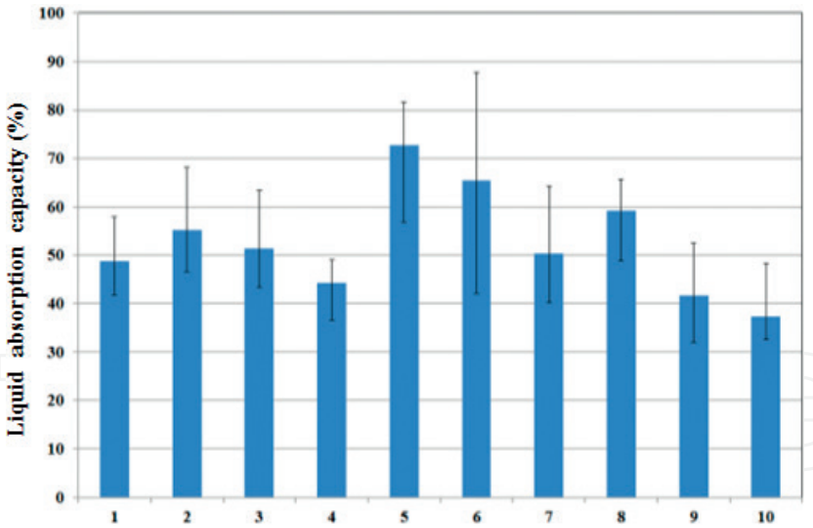

Figure 17.
Liquid absorption of specimens.

the thickness and weight, indicating that the nonwoven specimens with high thickness, high weight, and small pore size have a high sound absorption coefficient. In addition, these nonwoven specimens were made under manufacturing conditions of high needle depth or high blend ratio of LM PET. Lee and Joo [20] found that the sound absorption coefficient of nonwoven mixed with a large amount of fine fibers is high due to the friction of viscosity through the vibration of the air. Another study [21] attributed the increases in thickness and in the amount of the fiber per unit area to an increase in the sound absorption property of the nonwoven. These previous results were similar to our own.

3.1.5 Fogging property

A fogging test was carried out to determine the emission of volatile organic compounds (VOC) from automotive interior materials with increasing interior temperature during the summer time. **Figure 19** presents the fogging values of the nonwoven specimens. Specimen 1 treated with a single opener, specimen 4 treated with the one-time carding process, and specimen 5 treated with four layers of web showed high fogging values, whereas specimens 2, 6, and 8, with large mean pore size and high air permeability and water absorption, exhibited low fogging values. This was attributed to the easy flow of VOC gases developed from the nonwoven due to their large pores.

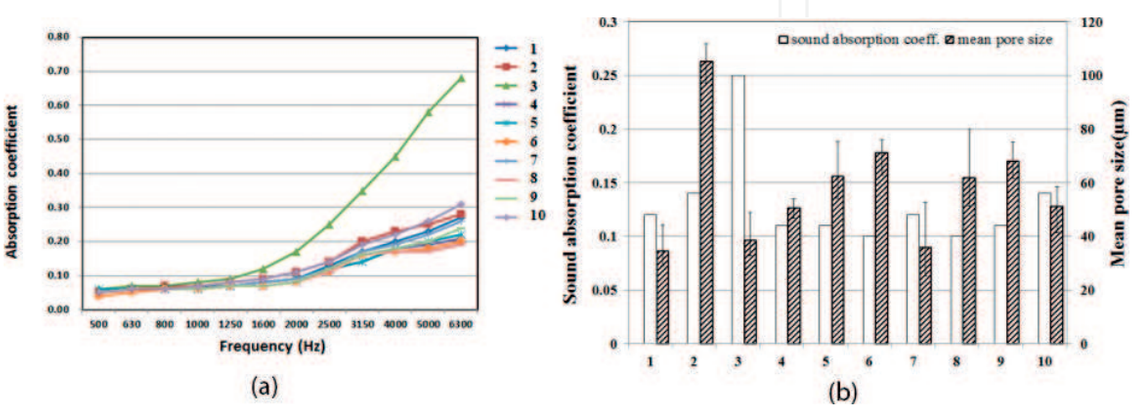

Figure 18.
Sound absorption coefficient of the nonwoven specimens. (a) Sound absorption coefficient and (b) Average sound absorption coefficients.

		Thickness (mm)	Weight (g/m^2)
Sound absorption coefficient	High frequency	0.91	0.83

Table 5.
Correlation coefficient between physical properties and sound absorption coefficient of nonwoven.

3.2 Physical properties of the kenaf-imbedded nonwoven according to powder treatment and laminated PU coating

3.2.1 Breaking and tearing strengths

Table 6 shows the physical properties of the kenaf-imbedded nonwoven specimens treated with powder and laminated by PU film, respectively.

Figure 20 presents the breaking and tearing strengths of the kenaf-imbedded nonwoven specimens treated and non-treated with laminated PU film. The breaking and tearing strengths of the laminated specimens were higher than those of the non-treated specimens, which was attributed to the PU film laminated on the nonwoven surface, resulting in higher weight and thickness. In addition, as shown in **Figure 20(b)** and **(d)**, the non-powder-treated specimens (6 and 8) exhibited higher breaking and tearing strengths than the powder-treated specimens (5 and 7), which were assumed to be weakened by adhesion between the PE powder and PU film by the heat on the laminating roller. On the other hand, as shown in **Figure 20(a)**, powder-treated specimens (1 and 3) exhibited higher breaking strength than the non-treated specimens (2 and 4), which was attributed to the enhancement of coherence between PE powder and LM PET fibers that were heat melted on the thermo-compression bonding roller.

Figure 21 presents a diagram of the fiber orientation of the nonlaminated nonwoven specimens (1–4). The degree of fiber orientation in the nonwoven was calculated as the mean of $\cos^2\theta$ of each specimens, i.e., unity of this value means orientation of fiber along the machine direction (MD) in the nonwoven, whereas zero value means fiber orientation along the cross direction (CD) in the nonwoven. Of these specimens, specimen 3 showed the highest value as a 0.46, and specimen 4 exhibited the lowest value as a 0.33, which resulted in the high difference between MD and CD in the breaking strength of this specimen 4 as shown in **Figure 20(a)** and **(c)**.

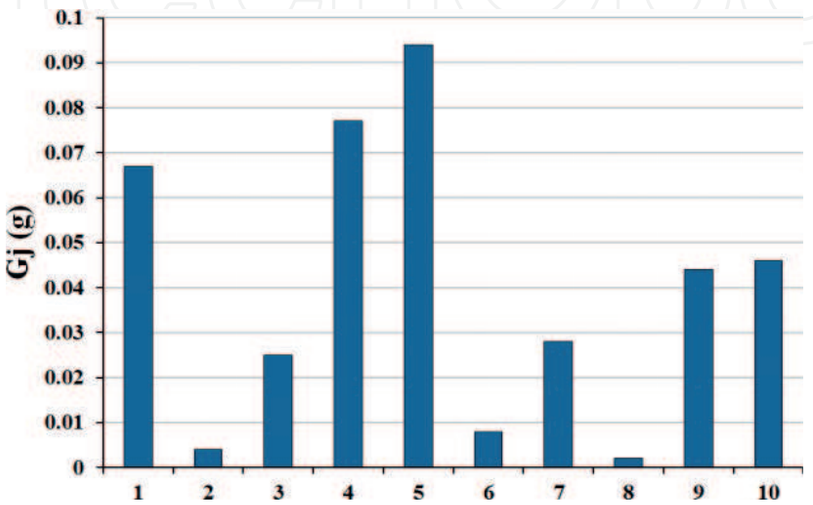

Figure 19.
Fogging values of the nonwoven specimens.

Specimen no.	Lamination	Powder treatment	Blend ratio (kenaf: PP:LM PET)	Mean pore size (mm)	Largest pore diameter (mm)	Strength				LAC (%)	Thermal conductivity (W/m°C)	Sound absorption coefficient		Air permeability ($cm^3/cm^2/s$)	Thickness (mm)	Weight (g/m^2)
						Breaking (kgf/mm^2)		Tearing (N)								
						MD	CD	MD	CD			Low freq.	High freq.			
1	Non-laminated	O	40:40:20	34.0	199.6	13.314	12.532	33.617	46.144	34.4	0.057	0.054	0.16	40.8	0.6	240
2		X	40:40:20	92.8	282.7	2.723	6.255	27.48	52.574	285.7	0.047	0.073	0.24	284.6	2.1	240
3		O	40:40:20	65.1	215.5	14.076	16.840	25.872	27.194	31.8	0.055	0.033	0.11	67.4	0.8	320
4		X	40:40:20	100.3	314.3	4.959	11.502	55.537	96.278	327.7	0.054	0.088	0.37	172.6	2.8	320
5	Laminated by PU film	O	40:40:20	35.9	117.8	27.412	26.753	106.832	97.39	25.3	0.056	0.055	0.24	63.2	1.3	420
6		X	40:40:20	59.0	180.7	35.534	31.763	127.353	163.11	177.2	0.061	0.096	0.42	98.5	2.5	420
7		O	40:40:20	49.2	196.5	31.253	26.458	138.78	103.013	20.6	0.056	0.082	0.33	27.6	1.5	500
8		X	40:40:20	83.8	230.1	40.715	24.136	142.402	200.036	253.6	0.059	0.128	0.54	88.6	3.2	500

Note: O, treated; X, non-treated.

Table 6.
Physical properties of the kenaf-imbedded nonwoven specimens (second batch of specimens).

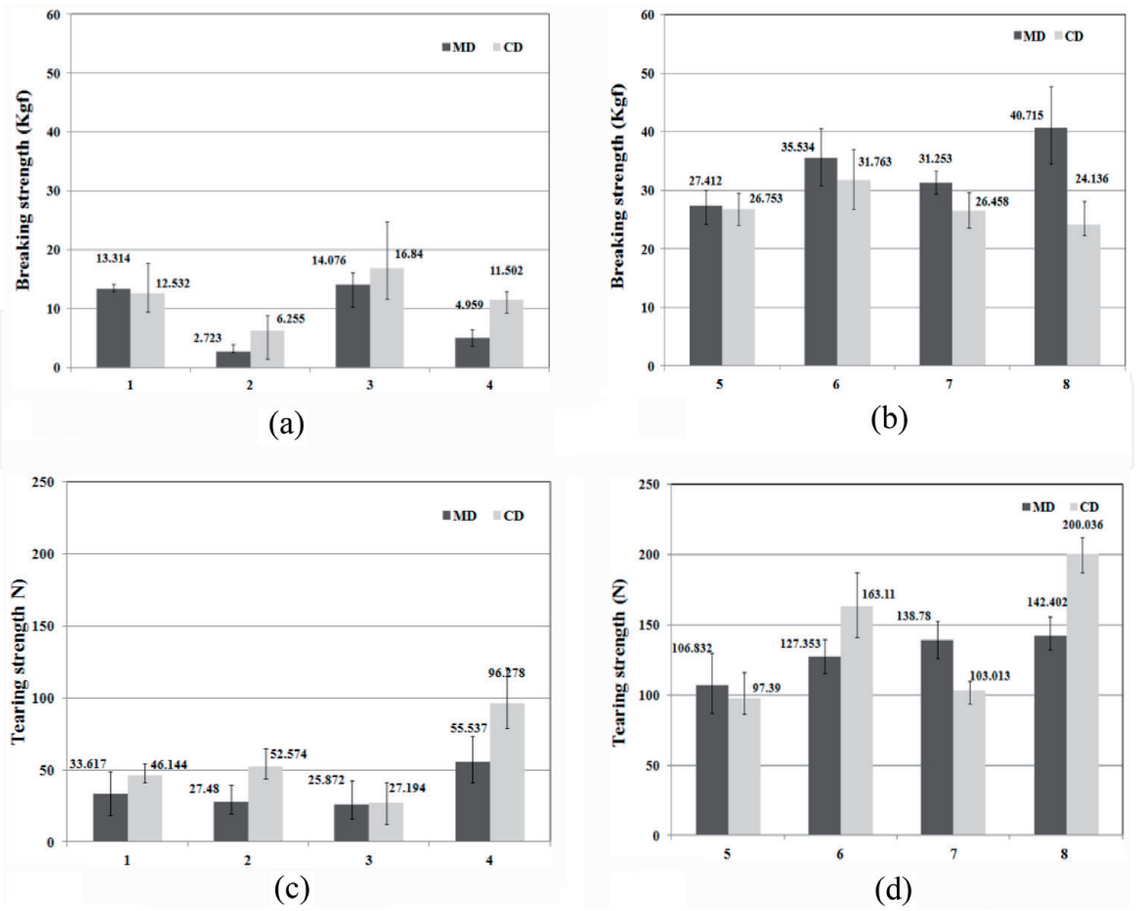

Figure 20.
Breaking and tearing strengths of the kenaf-imbedded nonwoven specimens (second group of specimens). (a) Breaking strength of nonlaminated specimens, (b) Breaking strength of laminated specimens, (c) Tearing strength of nonlaminated specimens and (d) Tearing strength of laminated specimens.

3.2.2 Air permeability and water absorption

Figure 22 shows the air permeability and water absorption of the kenaf-imbedded nonwoven specimens treated and nonlaminated with laminated PU film.

The differences of the air permeability and water absorption between the laminated and nonlaminated specimens were much lower than those between the

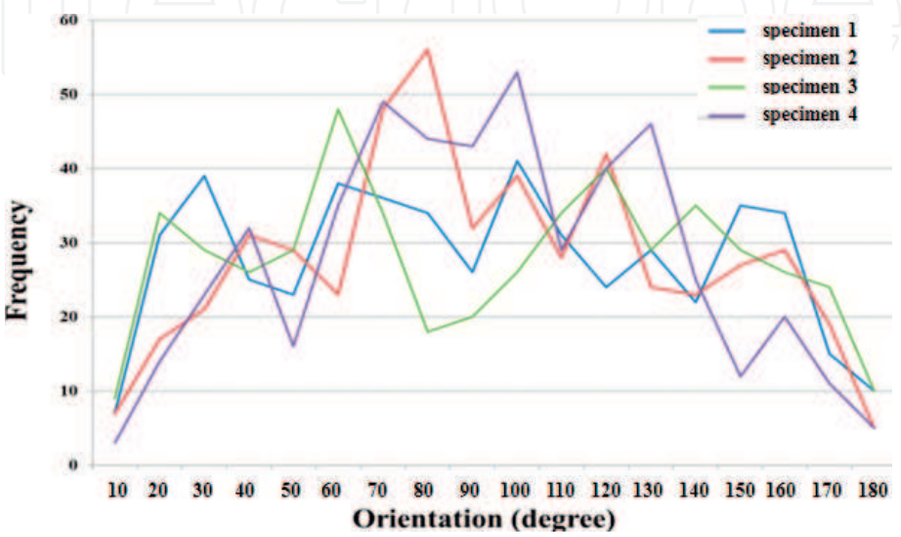

Figure 21.
Orientation of nonlaminated nonwoven specimens.

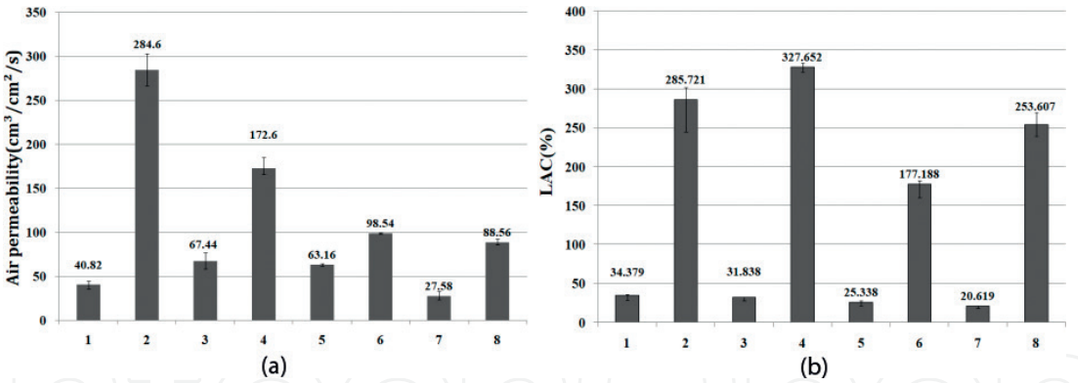

Figure 22.
Air permeability and water absorption of the kenaf-imbedded nonwoven treated and non-treated with laminated PU film. (a) Air permeability and (b) Water absorption.

powder-treated and non-treated specimens, i.e., the air permeability and water absorption of the non-powder-treated specimens (2, 4, 6, and 8) were much higher than those of the powder-treated specimens (1, 3, 5, and 7). Furthermore, the non-laminated specimens (1–4) exhibited higher air permeability and water absorption than did the laminated specimens (5–9). This was attributed to the small pore size of the powder-treated and laminated specimens, which was caused by the blockage of the pores in the nonwoven by melted powder in the thermo-compression bonding process and partly melted PU in the laminating process. This was verified by the mean pore and largest pore diameters of the kenaf-imbedded nonwoven specimens, as shown in **Figure 23**.

The mean pore and largest pore diameters of the non-powder-treated (2, 4, 6, and 8) and nonlaminated (1, 2, 3, and 4) specimens were much larger than those of the powder-treated (1, 3, 5, and 7) and laminated (5, 6, 7, and 8) specimens, respectively.

3.2.3 Thermal conductivity

Figure 24 shows the thermal conductivity of the kenaf-imbedded nonwoven specimens treated and non-treated with laminated PU film. The thermal conductivities of the powder-treated (1, 3, 5, and 7) and laminated (5–8) nonwoven specimens were higher than those of the non-powder-treated (2, 4, 6, and 8) and nonlaminated (1–4) specimens, respectively, which was attributed to less obstruction of heat particles' flow due to less air film in the smaller pores due to blockage of pores in the nonwoven by melted powder in the thermo-compression bonding process.

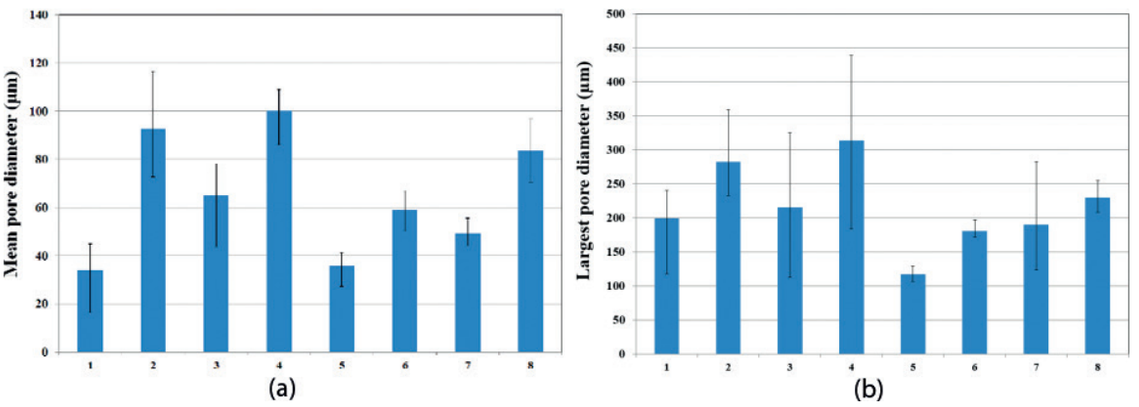

Figure 23.
Mean pore and largest pore diameters of the nonwoven specimens. (a) Mean pore dia and (b) Largest pore dia.

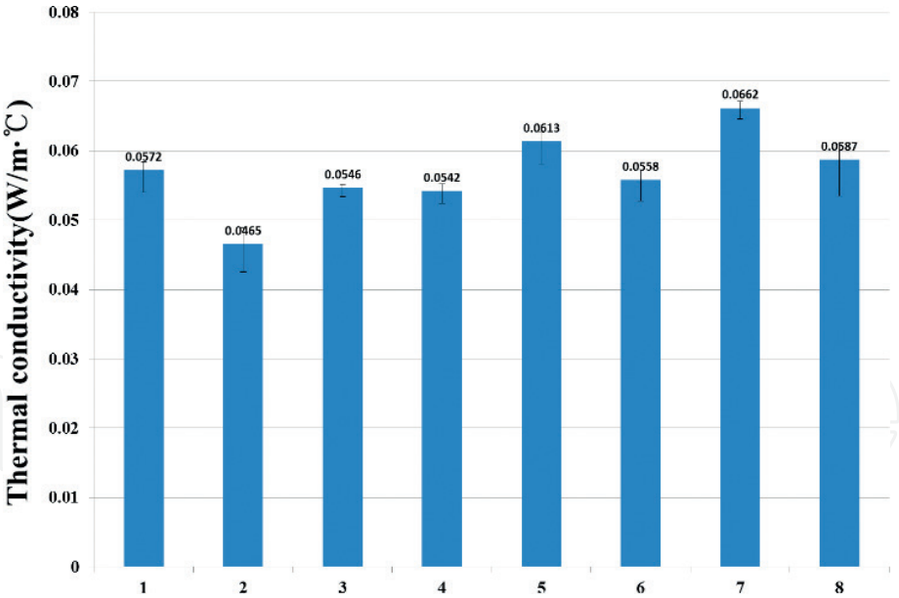

Figure 24.
Thermal conductivity of the laminated and nonlaminated nonwoven specimens.

3.2.4 Sound absorption

Figure 25 shows the sound absorption coefficients of the laminated and non-laminated nonwoven specimens at low and high frequencies. The sound absorption coefficients of the laminated specimens (5, 6, 7, and 8) were higher than those of the nonlaminated specimens (1, 2, 3, and 4), which was attributed to the increased thickness of the nonwoven due to the laminated film on its surface. Furthermore, the sound absorption coefficients of the powder-treated specimens (1, 3, 5, and 7)

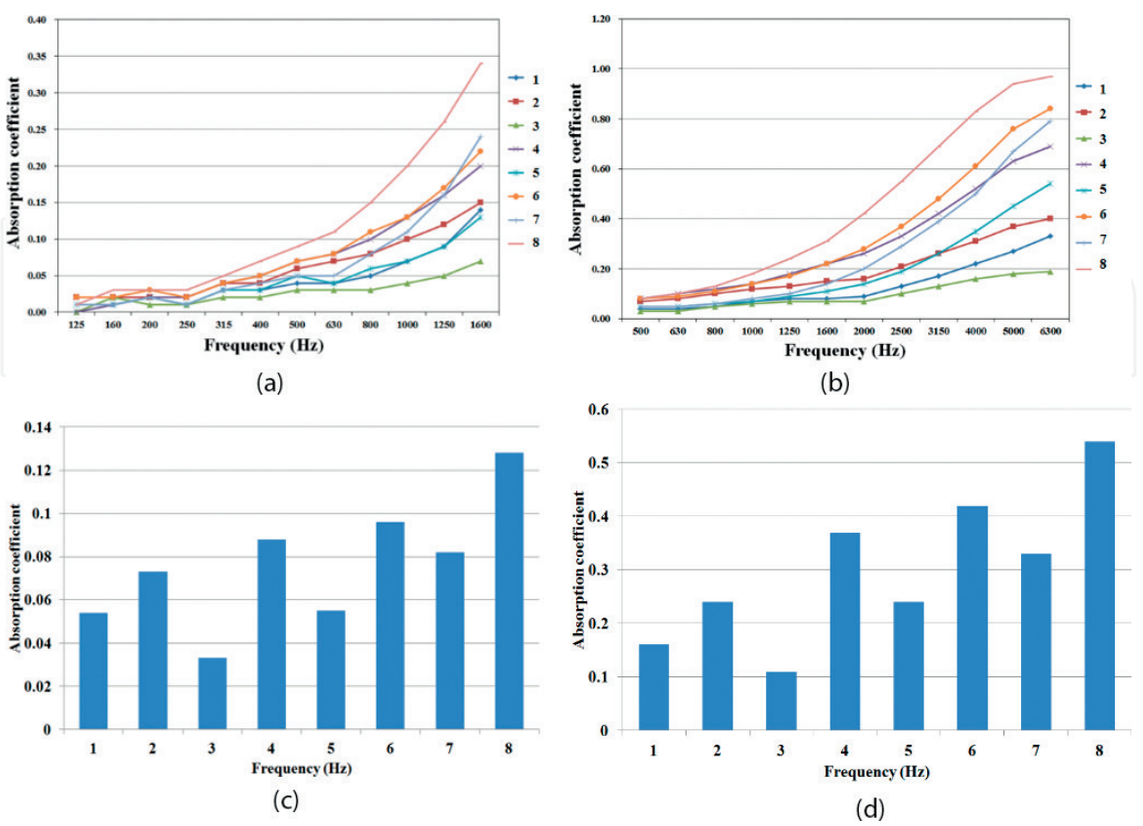

Figure 25.
Sound absorption coefficients of the kenaf-imbedded nonwoven specimens. (a) low frequency, (b) high frequency, (c) low frequency and (d) high frequency.

were lower than those of the non-treated ones (2, 4, 6, and 8), which was attributed to the thinner nonwoven and partly affected by its smaller pores due to blockage of the pores in the nonwoven by melted powder in the thermo-compression bonding process. In addition, the sound absorption coefficient of thick and heavy specimen 8, which was non-powder-treated and PU-laminated, was the highest, whereas those of thin and light specimens 1 and 3, which were powder-treated and non-PU-treated, exhibited lower value than others. The sound absorption coefficients of the laminated and nonlaminated nonwoven specimens according to the sound frequency during measurement exhibited a rapid increase around 630 Hz in the low-frequency experiment but showed a rapid increase around 1, 600 Hz in the high-frequency experiment.

3.2.5 Correlation between the physical properties and structural parameters of the kenaf-imbedded nonwoven specimens

Table 7 presents the correlation coefficient between physical properties and structural parameters of the kenaf-imbedded nonwoven specimens.

The breaking and tearing strengths of the kenaf-imbedded nonwoven specimens were highly correlated with weight of the nonwoven and inversely correlated with mean pore diameter in the kenaf-imbedded nonwoven and the orientation factor of its fibers. In particular, tensile property of the nonwoven according to the orientation factor exhibited a similar result to that of Rawal et al. [29]. The air permeability was highly correlated with the mean pore diameter as a porosity in the kenaf-imbedded nonwoven, which can be compared with those of the previous findings [26, 30]. The water absorption was also highly correlated with the mean pore diameter of the kenaf-imbedded nonwoven, and the thickness of the kenaf-imbedded nonwoven strongly affected its water absorption. This is in accordance with that of Das et al. [23]. They analyzed that more air trapped within the nonwoven with high porosity allows faster movement of water through pores. Furthermore, they suggested that this is in accordance with the theory of capillarity. The thermal conductivity of the nonwoven was dependent on its weight and was inversely correlated with its mean pore diameter. In addition, the sound absorption was highly correlated with thickness of the kenaf-imbedded nonwoven, and its

		Porosity		Thickness	Weight	Orientation factor
		Mean pore diameter (μm)	Largest pore diameter (μm)	(mm)	(g/m^2)	
Breaking strength		−0.55		0.25	0.88	−0.59
Tearing strength		−0.48		0.59	0.98	−0.55
Air permeability		0.85	0.49	0.44	−0.65	
Water absorption		0.91	0.68	0.84		
Thermal conductivity		−0.62			0.75	
Sound absorption	Low frequency	0.43	0.60	0.90	0.65	
	High frequency	0.41	0.48	0.91	0.83	

Table 7.
Correlation coefficient between physical properties and structural parameters of the kenaf-imbedded nonwoven specimens.

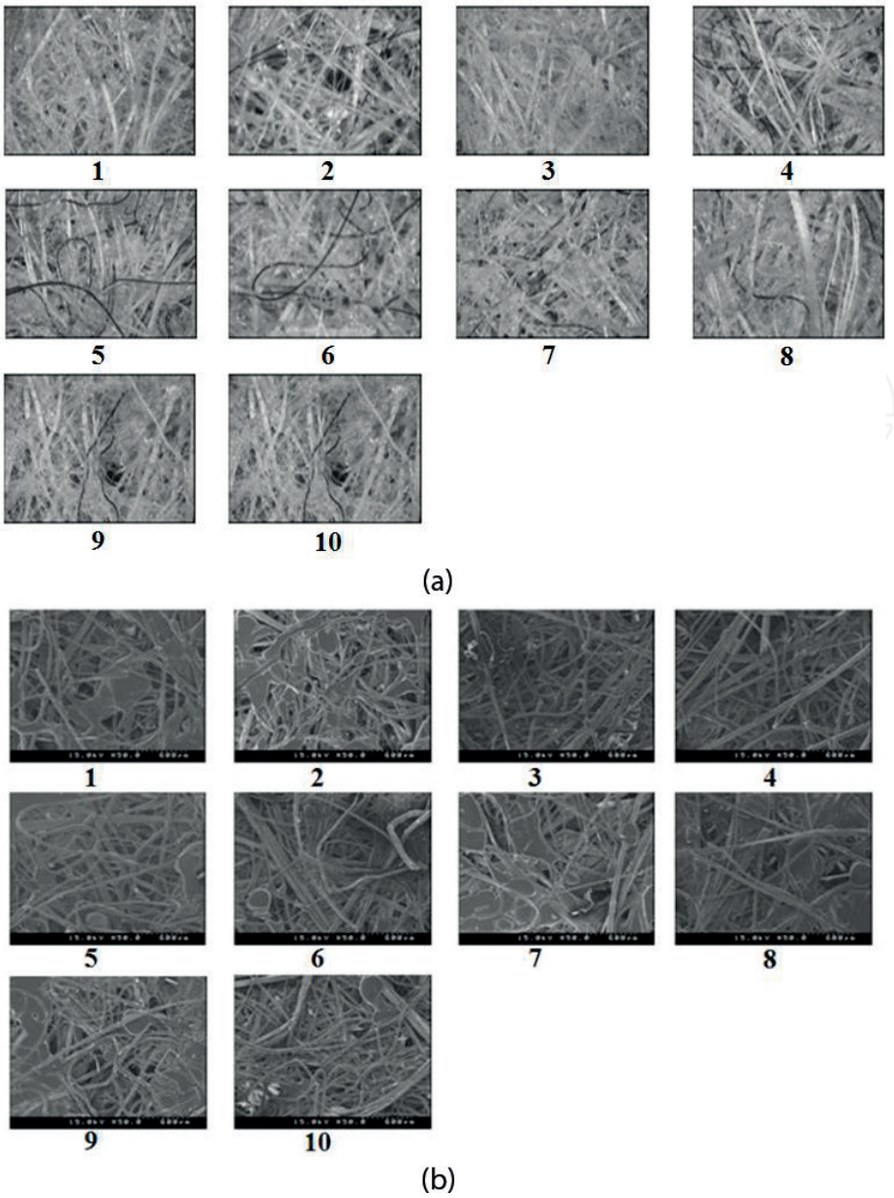

Figure 26.
Surface images of the kenaf-imbedded nonwoven specimens. (a) Optical microscopy (x100) and (b) SEM (x50).

weight affected the sound absorption, but its mean pore diameter did not. This was a similar result to those of previous studies [20, 21].

3.2.6 Surface images of the kenaf-imbedded nonwoven specimens

Figure 26 presents surface images of the kenaf-imbedded nonwoven specimens taken by SEM and optical microscopy.

The large pores observed for specimens 2, 6, and 9 resulted in high air permeability and water absorption, and these large pore diameters affected the breaking and tearing strengths. In addition, the thermal conductivity was inversely affected by the pore diameter. Specimens 1, 3, and 7 had small pore.

4. Conclusion

This study examined the relationship between the physical properties of kenaf-imbedded nonwoven and its structural factors according to the needle-punching

nonwoven processing conditions. The physical properties of kenaf fiber-imbedded nonwoven were measured and compared according to the blend ratio of the constituent fibers and the different nonwoven processing conditions. The results are summarized as follows.

The breaking and tearing strengths of the kenaf-imbedded nonwoven were dependent on its weight and its mean pore size. Nonwoven specimens with high needle depth and/or a large amount of LM PET exhibited high breaking and tearing strengths. The air permeability was highly dependent on the mean pore diameter of the kenaf-imbedded nonwoven. Nonwoven specimens processed with double carding, three layers of web, and with a needle depth of 16 mm exhibited high air permeability, which was due to high mean pore diameter and low weight. The water absorption of the kenaf-imbedded nonwoven was highly correlated with its mean pore diameter and thickness. A high blend percentage of LM PET fibers reduced the pore size, which resulted in low air permeability and water absorption. The sound absorption coefficient of the kenaf-imbedded nonwoven under high frequency was highly dependent on its thickness and weight and was also partly affected by the pore diameter, i.e., the kenaf-imbedded nonwoven with high thickness and weight exhibited a high sound absorption coefficient, and small-pore nonwoven showed a low sound absorption coefficient, manufactured with high needle depth and/or a high blend ratio of LM PET. In addition, the large-pore nonwoven specimen with high air permeability and water absorption exhibited a low fogging value, which was attributed to the easy flow of VOC gases developed from the nonwoven due to its large pores. Regarding the effects of powder and laminated PU treatment on the physical properties of the kenaf-imbedded nonwoven fabric, the breaking and tearing strengths of the laminated specimens were higher than those of the nonlaminated specimens, and the non-powder-treated specimens exhibited higher breaking and tearing strengths than the powder-treated specimens after PU laminating. The air permeability and water absorption of the non-powder-treated specimens were much higher than those of the powder-treated specimens. Moreover, the laminated and non-powder-treated specimens exhibited higher sound absorption coefficient than did the nonlaminated and powder-treated specimens. On the other hand, the thermal conductivities of the powder-treated and PU-laminated specimens were higher than those of the non-powder-treated and nonlaminated ones.

Author details

Seung Jin Kim[1*] and Hyun Ah Kim[2]

1 Department of Fiber System Engineering, Yeungnam University, Gyeongsan, Korea

2 Korea Research Institute for Fashion Industry, Daegu, Korea

*Address all correspondence to: sjkim@ynu.ac.kr

References

[1] Ramaswamy GN, Craft S, Wartelle L. Uniformity and softness of kenaf fibers for textile products. Textile Research Journal. 1995;**65**:765-770. DOI: 10.1177/004051759506501210

[2] Tao W, Moreau JP, Calamari TA. Properties of nonwoven mats from kenaf fibers. Technical Association of Pulp & Paper. Industry Journal. 1995;**78**:165-169

[3] Lee H, Ahn C, Kim J, Yoo H, Han Y, Song K. The characteristics of kenaf/rayon fabrics. Journal of the Korean Society of Clothing and Textiles. 2004;**20**:1282-1291

[4] Lee H, Yoo H, Han Y. The properties of kenaf/polyester blended nonwovens. Journal of the Korean Society of Clothing and Textiles. 2007;**31**:1696-1706

[5] Bel-Berger P, Hoven TV, Ramaswamy GN, Kimmel L, Boylston E. Textile technology cotton/kenaf fabrics: A viable natural fabrics. The Journal of Cotton Science. 1999;**3**:60-70

[6] Weiying T, Calamari TA. Preparing and characterizing kenaf/cotton blended fabrics. Textile Research Journal. 1999;**69**:720-724

[7] Zhang X. Investigation of biodegradable nonwoven composite based on cotton, bagasse and other annual plants [thesis]. Louisiana: Louisiana State University; 2004

[8] Jung JS, Song KH, Kim SH. Mechanical properties and biodegradability of enzyme-retted kenaf fiber composites. Textile Research Journal. 2018. DOI: 10.1177/0040517518779996

[9] Dunne R, Desai D, Sadiku R, Jayaramudu J. A review of natural fibers, their sustainability and automotive applications. Journal of Reinforced Plastics & Composites. 2016;**35**:1041-1050

[10] Thilagavathi G, Pradeep E, Kannaian T, Sasikala L. Development of natural fiber nonwovens for application as car interiors for noise control. Journal of Industrial Textile. 2010;**39**:267. DOI: 10.1177/1528083709347124

[11] Moreau JP, Bel-Berger P, Tao W. Mechanical Processing of Kenaf for Nonwovens. Tappi Journal. 1995;**78**:96-105

[12] Yang JQ, Morisawa J, Sameshima YQ. Kenaf bast fiber treatment for nonwoven fabrics. Sen'l Gakkaichi. 2001;**57**:88-93

[13] Tao W, Calamari TA, Shih FF, Cao C. Characterization of kenaf fiber bundles and their nonwoven mats. Tappi Journal. 1997;**80**:162-166

[14] Tao W, Calamari TA, Crook L. Carding kenaf for nonwovens. Textile Research Journal. 1998;**68**:402-406. DOI: 10.1177/004051759806800603

[15] Fatima S, Mohanty AR. Acoustical and fire-retardant properties of jute composite materials. Applied Acoustic. 2011;**72**:108-114. DOI: 10.1016/j.apacoust.2010.10.005

[16] Fouladi MH, Ayub M, Nor MJM. Analysis of coir fiber acoustical characteristics. Applied Acoustic. 2011;**72**:35-42. DOI: 10.1016/j.apacoust.2010.09.007

[17] Parikh VD, Chen Y, Sun L. Reducing automotive interior noise with natural fiber nonwoven floor covering systems. Textile Research Journal. 2006;**76**:813-820. DOI: 10.1177/0040517506063393

[18] Nick A, Becker U, Thoma W. Improved acoustic behavior of interior

parts of renewable resources in the automotive industry. Journal of Polymers and the Environment. 2002;**10**:115-118. DOI: 10.1023/A:1021124214818

[19] Lou CW, Lin JH, Su KH. Recycling polyester and polypropylene nonwoven selvages to produce functional sound absorption composites. Textile Research Journal. 2005;**75**:390-394. DOI: 10.1177/0040517505054178

[20] Lee YN, Joo CW. Sound absorption properties of recycled polyester fibrous assembly absorbers. AUTEX Research Journal. 2003;**3**:78-84

[21] Byun HS, Lee TG. A study on the characteristic of sound absorption of the polyester non-woven fabrics used for the automobile sound absorption material. POLYMER-KOREA. 2001;**25**:427-434

[22] Kücük M, Korkmaz Y. The effect of physical parameters on sound absorption properties of natural fiber mixed nonwoven composites. Textile Research Journal. 2012;**82**:2043-2053. DOI: 10.1177/0040517512441987

[23] Dubrovski PD, Brezocnik M. Porosity and nonwoven fabric vertical wicking rate. Fibers and Polymers. 2016;**17**:801-808. DOI: 10.1007/s12221-016-6347-5

[24] Soukupova V, Boguslavsky L, AnandJiwala RD. Studies on the properties of biodegradable wipes made by the hydroentanglement bonding technique. Textile Research Journal. 2007;**77**:301-311

[25] Dubrovski PD, Brezocnik M. The modelling of porous properties regarding PES/CV-blended nonwoven wipes. Fibers and Polymers. 2012;**13**:363-370. DOI: 10.1177/0040517507078239

[26] Das D, Ishtiaque SM, Das S. Influence of fiber cross-sectional shape on air permeability of nonwovens. Fibers and Polymers. 2005;**16**:79-85. DOI: 10.1007/s12221-015-0079-9

[27] Tascan M, Vaughn EA. Effects of total surface area and fabric density on the acoustical behavior of needlepunched nonwoven fabrics. Textile Research Journal. 2008;**78**:289-296. DOI: 10.1177/0040517507084283

[28] CSIRO Division of Wool Technology. The FAST system for the objective measurement of fabric properties. Operation. Interpretation and Application, CDW Technology. Geelong, Australia; 1989

[29] Rawal A, Lomov S, Ngo T, Verpoest I, Vankerre brouck J. Mechanical behavior of thru-air bonded nonwoven structures. Textile Research Journal. 2007;**77**:417-431

[30] Das D, Ishtiaque SM, Ajab Rao SV, Pourdeyhimi B. Modelling and experimental studies of air permeability of nonuniform nonwoven fibrous porous media. Fibers and Polymers. 2013;**14**:494-499